ARTICLE

Assessing the size spectra of marine fish communities with hydroacoustics: examining the challenges of abundant schools, diverse assemblages, and variable orientations

Derek G. Bolser, Jack P. Egerton, Philip M. Souza, Jr., Kevin M. Boswell, and Brad E. Erisman

Abstract: Assessing marine fish community size spectra with hydroacoustics is challenging, as communities are diverse, schooling and swim-bladder-less fishes are common, and fish orientation is variable. We developed an approach to examine these challenges and applied it to data from 51 optic–acoustic surveys of fishes at petroleum platforms throughout the US Gulf of Mexico. When in situ target strength (TS; dB re 1 m^2) distributions were used to calculate the density (and subsequently abundance) of schooling fishes, fish lengths and size spectra slopes were significantly smaller than in simulated communities and fish community censuses at platforms (i.e., reference datasets). However, acoustic slopes were comparable to reference slopes when simulated TS values (based on species composition) were used to calculate schooling fish abundance. These findings held regardless of whether specific or general models were used to convert TS to length. Fish orientation was not a useful predictor of TS or slope, but may explain why in situ TS measurements from small groups of fishes around schools were unsuitable for abundance calculations. By examining the challenges associated with assessing size spectra with acoustics, this study aids progress towards using acoustic size spectra metrics for ecological inferences.

Résumé : L'évaluation des spectres de tailles de communautés de poissons marins par des méthodes hydroacoustiques est difficile, en raison de la diversité de ces communautés, du fait qu'il y a souvent des poissons en bancs et des poissons sans vessie natatoire et de l'orientation variable des poissons. Nous présentons une approche permettant d'examiner ces difficultés et l'appliquons aux données de 51 relevés optiques-acoustiques de poissons autour de plateformes pétrolières réparties dans toute la portion américaine du golfe du Mexique. Quand les distributions des indices de réflexion (TS; dB re 1 m^2) in situ sont utilisées pour calculer la densité (et ensuite l'abondance) des poissons en banc, les longueurs de poissons et les pentes des spectres de tailles sont significativement plus faibles que les valeurs pour les communautés simulées et issues de recensements des communautés de poissons autour de plateformes (c.-à-d. des ensembles de données de référence). Les pentes acoustiques sont toutefois semblables aux pentes de référence quand des valeurs de TS simulées (basées sur la composition spécifique) sont utilisées pour calculer l'abondance de poissons en banc. Ces constatations persistent peu importe si des modèles spécifiques ou généraux sont utilisés pour la conversion de TS en longueur. L'orientation des poissons n'est pas un prédicteur utile du TS ou de la pente, mais pourrait expliquer pourquoi les mesures in situ du TS de petits groupes de poissons autour de bancs ne se prêtent pas au calcul de l'abondance. En examinant les difficultés associées à l'évaluation des spectres de tailles par des méthodes acoustiques, l'étude constitue un pas de plus vers l'utilisation de mesures acoustiques des spectres de tailles pour établir des inférences écologiques. [Traduit par la Rédaction]

Introduction

Communities of aquatic organisms are typically structured as pyramids in which many small individuals support fewer larger individuals, and the relationship between abundance and size may be described by a power law function (Elton 1946; Trebilco et al. 2013; Sprules and Barth 2016). These abundance pyramids — and the inverted pyramids describing biomass distribution — may be represented as size spectra, which are often quantitatively assessed by regressing logged abundance or biomass against logged bins of length or biomass (Trebilco et al. 2013; Sprules and Barth 2016;

Edwards et al. 2017). Size spectra slopes can also be estimated by fitting a probability density function to size distribution data to remove biases associated with binning (Edwards et al. 2017). One of the most informative metrics coming from this type of analysis is the slope of the regression line or probability distribution, which describes how the abundance or biomass of small organisms compares to the abundance or biomass of large organisms (Bianchi et al. 2000; Daan et al. 2005; Sweeting et al. 2009).

The size spectrum of an aquatic community reflects energy flow between trophic levels and the ecological processes that shape it (Trebilco et al. 2013; Sprules and Barth 2016). As such, the

Table 1. Simple definitions, abbreviations, and units for acoustics-related terminology as they are used in this paper.

Term	Abbreviation or symbol, unit	Simple definition
Split-beam hydroacoustics	Acoustics	"Active" acoustic technology in which a transducer emits a pulse of sound (i.e, "ping") into the water column and records the reflected reverberation (i.e., "backscatter"). The transducer elements are split into quadrants, which facilitates target tracking and measurements of fish orientation and change in range
Volume backscattering strength	S_v, dB re 1 m^{-1}	Mean backscattered acoustic energy measured in a volume of water
Volume backscattering coefficient	s_v, m^{-1}	Volume backscattering strength in the linear domain
Target strength	TS, dB re 1 m^2	Backscattered acoustic energy that is attributed to a single target
Backscattering cross-section	σ_{bs}, m^2	Target strength in the linear domain
In situ target strength	In situ TS, dB re 1 m^2	Target strength measurements made in the field, as opposed to measurements made in the laboratory, simulated measurements, or measurements converted from lengths
Single target	—	An individual fish detected with acoustics
Tracked fish	—	An individual fish whose reverberated acoustic energy has been recorded in multiple successive pings
School	—	Dense group of fishes in which single targets or tracked fishes cannot be isolated
Ground-truthing data	—	Data that are complementary to acoustic data. These data are required to assign taxonomic information to acoustic data, and depending on the type of data, corroborate estimates of length derived from converting TS to length
Orientation	Degrees	The tilt angle of a fish relative to the acoustic transducer

Note: Information follows MacLennan et al. (2002) and Simmonds and MacLennan (2008), which we refer the reader to for more complete definitions and further details.

size spectra concept has been used to understand food web structure, macroecology, and the influence of environmental stressors or anthropogenic activities on aquatic communities (Wilson et al. 2010; Blanchard et al. 2017; Heneghan et al. 2019). For example, fishing preferentially removes larger individuals and species (Mason 1998; Jennings and Kaiser 1998; Berkeley et al. 2004), resulting in steepening (i.e., more negative) size spectra slopes for fish communities over time and increasing fishing activity (Pope and Knights 1982; Blanchard et al. 2009; Robinson et al. 2017). The size spectra of fish communities may also reveal differences in ecosystem productivity, with communities in areas of high productivity exhibiting steep size spectra slopes due to a high relative abundance of small, planktivorous fishes (Emmrich et al. 2011; Secor 2015). Since size is thought to be the primary determinant of many biological processes in marine organisms (Andersen et al. 2016), size-based community metrics, such as the slope of the size spectrum, are attractive for application in Ecosystem-Based Fisheries Management (Jennings and Dulvy 2005; Shin et al. 2005).

Due to its noninvasive nature and limited selectivity bias compared to other methods, split-beam hydroacoustics (Table 1; hereinafter "acoustics") represents a promising tool for rapidly collecting the data necessary to assess the size spectra of fish communities (Trenkel et al. 2011). Acoustics has been applied successfully to assess the size spectra of fish communities in freshwater systems (e.g., Yurista et al. 2014; Wheeland and Rose 2016; de Kerckhove et al. 2016), although the results of validation studies that compared acoustically derived size spectra with size spectra estimated with other gears have been inconsistent (Coll et al. 2007; de Kerckhove et al. 2016; Daigle 2017). Acoustic technology is not commonly applied to assess the size spectra of marine fish communities, as doing so involves dealing with significant assumptions and uncertainties related to the diverse assemblages and behaviors of marine fishes (Egerton 2017). The potential benefits of using acoustics to study the size spectra of marine fish communities (e.g., noninvasive, rapid assessments) make efforts to address these challenges worthwhile.

Perhaps the greatest challenge in assessing fish size spectra with acoustics is relating target strength (Table 1; TS, dB re 1 m^2) to fish length (Simmonds and MacLennan 2008). Acoustic size spectra studies typically employ an empirically derived general TS–length relationship across species (e.g., Yurista et al. 2014;

Wheeland and Rose 2016; de Kerckhove et al. 2016). However, converting TS to length is most accurate when a specific model is developed for each species of fish observed, as fish swim bladder morphology (or lack of swim bladder) greatly influences TS (Foote 1980; McClatchie et al. 1996a; Simmonds and MacLennan 2008). Specific models do not exist for many common species in marine environments, and though applying species-specific TS–length relationships to species other than the species for which the model was derived is generally not advisable (Foote 1979; McClatchie et al. 1996a), some species within some families may exhibit similar scattering properties (e.g., Benoit-Bird et al. 2003; Boswell et al. 2020). Even so, the coexistence of swim-bladdered and bladder-less fishes that is often observed in marine environments complicates the application of TS–length models, as TS distributions may overlap between small swim-bladdered fishes and larger bladder-less fishes.

Relating TS to fish length is further complicated by the effect of fish orientation, relative to the transducer face, on variation in measured backscatter. Since fishes with varying orientations relative to the transducer present different cross-sections of their swim bladder (or body for bladder-less fishes), the measured TS of a fish can vary significantly (Nakken and Olsen 1977; McClatchie et al. 1996b; Simmonds and MacLennan 2008). It is possible to collect data on the orientation of fishes by acoustically tracking them through successive "pings" (Table 1), but incorporating the effect of orientation in TS–length models can be challenging. There are few TS–length models that account for orientation (e.g., Kubečka 1994; Lilja et al. 2000; Johnson et al. 2019), so the influence of fish orientation on size spectra metrics must be investigated through simulations (de Kerckhove et al. 2016) and statistical comparisons.

The presence of schooling fishes also affects the ability of acoustics to describe the size spectra of fish communities. In most schools, it is not possible to isolate valid single targets or tracked fishes (Table 1). Accordingly, the TS of individual fishes cannot be measured, and assumptions must be made to estimate the TS distribution and number of fishes within schools. In many acoustic studies, ground-truthing data (Table 1) are collected through direct capture approaches (e.g., de Blois 2020), but this approach is not possible in all habitat types. Another approach is to use in situ TS measurements

Fig. 1. Overview of the process of estimating size spectra with hydroacoustics with common issues, sensitivity analyses to address those issues, and guidance. [Colour online.]
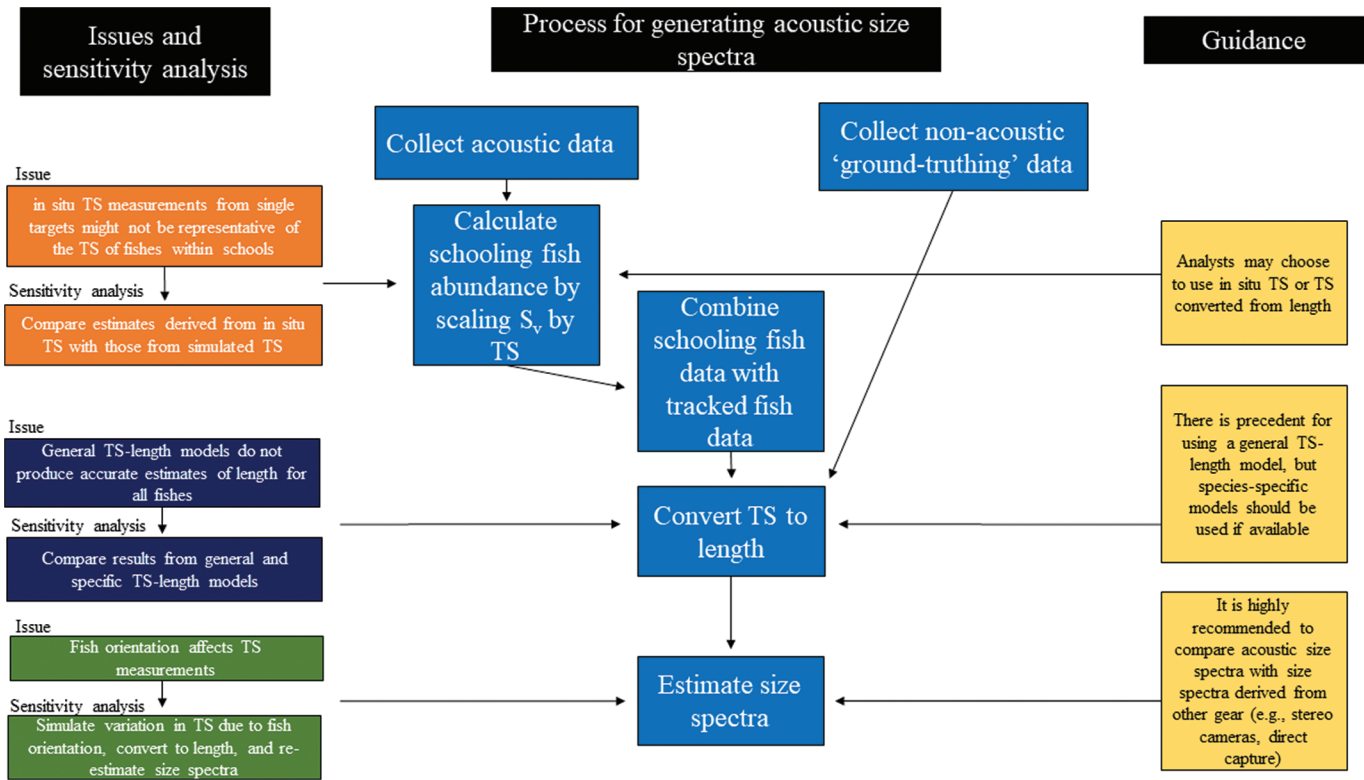
(Table 1) to represent the mean or distribution of TS within a school for scaling school volume backscattering strength (Table 1; S_v, dB re 1 m^{-1}) to fish density and subsequently abundance (e.g., MacLennan 1990; Boswell et al. 2010; Scoulding et al. 2017). However, it is not possible to test if the TS of surrounding single targets is representative of the TS of fishes within schools with acoustic data alone. At present, the degree to which specifying the TS distribution of schools in different ways affects acoustic size spectra estimates is unknown.

To evaluate the challenges associated with using acoustics to estimate the size spectra of marine fish communities, we (1) compared size spectra slopes and fish lengths derived from acoustic data with those derived from published fish community censuses and simulated communities based on species composition (i.e., reference datasets), including an evaluation of the impact of using different sources of TS data for scaling school S_v (in situ TS distributions vs. simulated TS distributions based on three different scenarios for species composition); (2) examined the impact of using general or species-specific TS–length models on size spectra slopes and fish lengths; and (3) quantified the effect of tracked fish orientation on TS and size spectra slopes. We present our approach in a generalized manner and describe its application to an optic–acoustic dataset collected at petroleum platforms in the US Gulf of Mexico (GOM). This investigation of acoustic size spectra is the first to consider the effect of different treatments of school S_v and TS, compare results derived from general and specific TS–length models, and place the associated variability in the context of other known effects on acoustic size spectra (e.g., fish orientation). By quantitatively examining sources of bias, uncertainty, and variability in a dataset of diverse reef fish communities, the present study represents an important step towards operationalizing acoustic size spectra metrics for ecological inferences.

Methods

Overview

Here, we explain our methodology for assessing the impact of different treatments of acoustic data on size spectra slopes (Fig. 1) to address the goals and challenges stated above. The approach we describe can be applied in situations where both schooling and tracked fishes are detected in acoustic data and ground-truthing data are available to address similar goals. We describe our application of this methodology to an optic-acoustic data collected at petroleum platforms in US waters of the GOM and outline how we compared results derived from those data with reference datasets. In total, we compared 7 datasets: 5 in which fish length information was derived from acoustics or a combination of acoustics and simulations and 2 in which length information was derived from field collections or simulations (i.e., reference datasets; Fig. 2). To facilitate easier interpretation of acoustic methodology, we listed simple definitions, abbreviations, and units for acoustic-related terminology in Table 1.

We first present the generalizable methodology that we used to generate the 5 datasets in which acoustics, or a combination of acoustics and simulations, were used to estimate fish length and estimate size spectra (Figs. 1, 2). We begin with describing four options for calculating the abundance of schooling fishes at each site that were designed to represent different scenarios for the species and size composition of schooling fishes (Fig. 2). These four options consisted of using either in situ TS measurements or three different ranges of simulated TS values to scale the S_v of schools to fish abundance (Fig. 2). After schooling fish abundance is estimated at each site via each of the four options (comprising separate datasets for each option), the schooling fish data are combined with tracked (i.e., non-schooling) fish data for each site in each dataset. Every fish at every site in each dataset is associated with an estimate of TS, which is converted to length in one

1258

Can. J. Fish. Aquat. Sci. Vol. 79, 2022

Fig. 2. Simplified workflow for estimating the abundance of fishes, generating the datasets analyzed in this study, and terminology used to describe the datasets. [Colour online.]
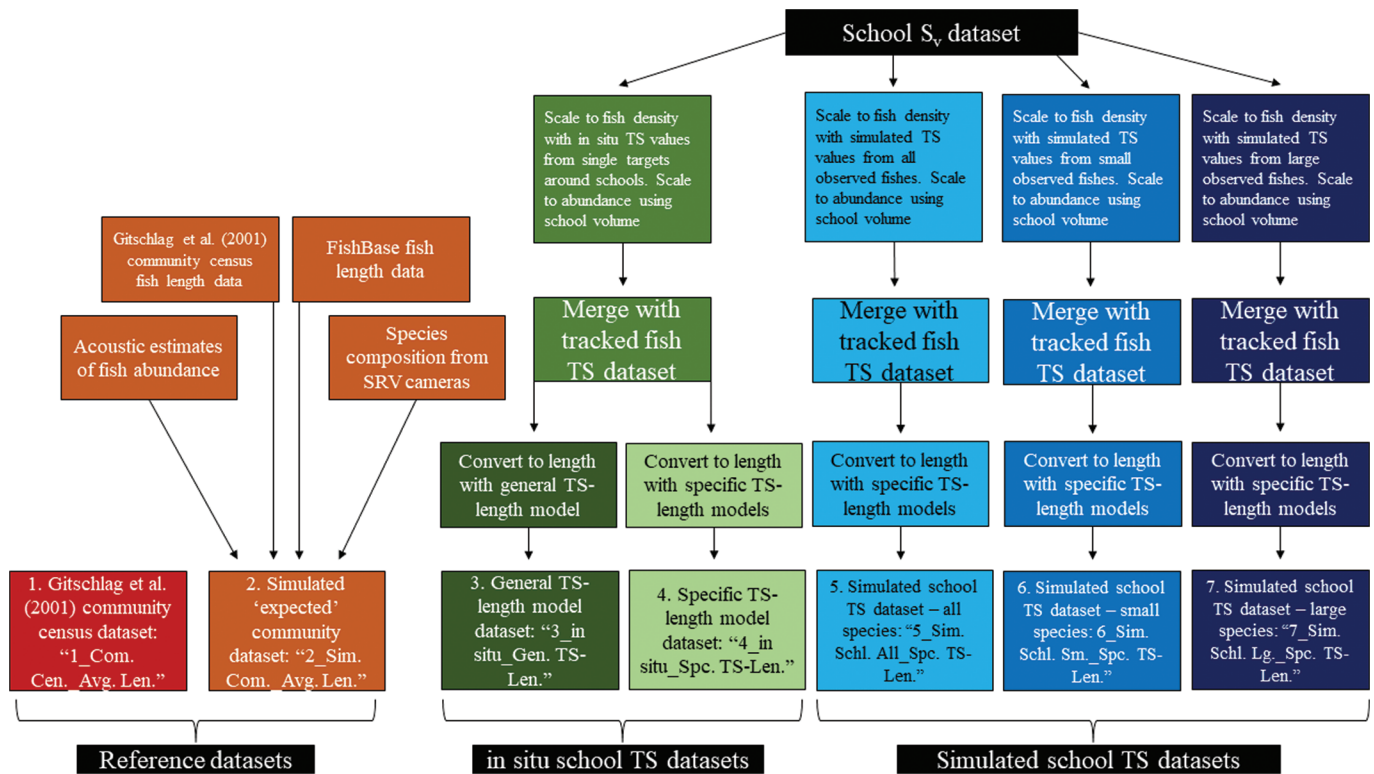
of two ways — one of which requires information about species composition (conducted in all datasets), the other of which does not (conducted for the in situ school TS dataset; Fig. 2). This process results in a complete representation of the lengths of all fishes at every site in each dataset that were sampled by acoustics and five datasets total (four in which TS was converted to length with specific TS–length models, one in which TS was converted to length with a general TS–length model; Fig. 2). With these data, we then calculate size spectra slopes for the fish communities sampled by acoustics at each site in each dataset. We conclude our generalizable methodology by describing four ways for calculating the influence of fish orientation on TS and size spectra slopes.

For our application of this methodology, we describe how optic and acoustic data were collected at petroleum platforms throughout the US GOM and how our two reference datasets were generated. We also explain how we adapted our generalizable methodology to our specific data, including the parameters of our simulations and which specific TS–length models were used in our example. Finally, we describe the statistical comparisons we made between results derived from different acoustic and reference datasets.

Calculation of fish abundance within schools: 4 scenarios

We developed four different scenarios for relating school S_v to the abundance of fishes within schools (summarized in Fig. 2) at each site. In the first, the S_v of schools is scaled by the in situ TS distribution of single targets around them (1–3 m from the school boundary, or the nearest possible values if none existed within that range) to calculate fish density. Then, density estimates are converted to abundance using the volume of the school. This procedure is conducted in the following manner:

$$(1) \quad N = \sum_n^i \frac{s_v}{\sigma_{bs_i}}(p_i V)$$

where N is the number of fishes in a given school, s_v is the volume backscattering coefficient (Table 1), σ_{bs_i} is the backscattering cross-section (Table 1) of single targets around the school in 3-dB bin i, p_i is the proportion of single target observations around the given school within TS bin i (relative to the total number of single targets around the school), and V is the volume of the school. The midpoint of each 3-dB bin is used to represent the TS of single targets within the bin. Following the abundance calculation, each fish is assigned the value of σ_{bs_i} that was used to estimate abundance in the proportion of school volume that the fish came from. In calculating fish density with TS values from single targets around the school, we assume that single targets around schools are representative of targets within schools. As described below, we also investigated alternate assumptions.

In the other three scenarios, the same procedure can be used to calculate the abundance of fish in schools. However, the TS values used to scale the S_v of the school differs. In each scenario, a simulated value of TS is generated for each single target around a given school observed in the acoustic data. The parameters of the simulation differ between the scenarios, which were designed to represent three possible situations based on species compositions and fish behavior: (1) single targets around schools were composed of all species observed in ground-truthing data, (2) single targets around schools were composed of the small pelagic species that typically form dense fish schools, and (3) single targets around schools were composed of large piscivorous species that may prey upon the small pelagic schooling species. In the first of these scenarios, TS values are simulated from a truncated normal distribution centered around the mean expected TS of all species observed in ground-truthing data. Expected TS is estimated by converting lengths from the ground-truthing data using species-specific TS–length models (described in greater detail in the subsequent section). The distribution is truncated by a lower value of the smallest expected TS in the ground-truthing data, and an

upper value of the largest expected TS in the ground-truthing data. The standard deviation of the distribution is set to the standard deviation of expected TS among all species in the ground-truthing data. Accordingly, our procedure simulates a TS value for each single target around each school from a distribution informed by the expected TS values of all species observed. The procedure for assigning species identities to each TS observation after abundance estimation for the purposes of TS–length conversion is described below in the section "Conversion of TS to length".

The same procedure can be followed to generate TS values for single targets around schools in the remaining scenarios, but using only expected TS values for small pelagic species in the second of these scenarios and only expected TS values for large piscivorous species in the third. These scenarios were developed to evaluate the consequences of scaling school S_v with TS observations from species that may not have been represented within dense schools, yet were encountered in the surrounding area.

Following abundance estimation and TS assignment in every scenario, the schooling fish data (i.e., the total abundance and TS distribution of schooling fishes) is added to data from tracked fishes (i.e., the total abundance and TS distribution of non-schooling fishes) that were recorded by the echosounder and detected with a fish tracking algorithm (explained in detail below in the section "Acoustic data processing") to form a dataset of the total abundance and TS distribution of fishes sampled by the echosounder (i.e., water column fishes) at each site. This procedure is conducted separately for each study site in each scenario.

Conversion of TS to length: general and specific models

The TS of fishes can be converted to length in two ways to identify the impact of TS–length model choice on size spectra slopes. For the first approach to converting TS to length, the general TS–length model of Love (1971) is applied to all data to represent a situation in which no ground-truthing data were available and the species sampled were unknown. The TS–length model of Love (1971) for 120 kHz transducers is

$$(2) \qquad \text{Length} = 10^{\text{TS}+63.85/19.1}$$

For the second approach to converting TS to length, specific TS–length models are chosen based on the identity of the species recorded in ground-truthing data. To apply these models, it is necessary to assign a species identity to each TS observation. This is done by (1) converting length from ground-truthing data for each species to TS using the closest published TS–length formula for the observed species; (2) ordering the species from smallest to largest predicted TS value and similarly ordering the TS dataset from smallest to largest for each survey; (3) proportionally assigning TS observations a species identity in order based on the observed relative abundance of species; and (4) applying TS–length models to TS values by their assigned species to estimate lengths.

Estimation of size spectra slopes

Size spectra slopes for each site in each dataset can be calculated following the maximum likelihood estimation method of Edwards et al. (2017). Briefly, the slope of a bounded power law distribution fit to size distribution data are estimated in this method, rather than binning data and estimating size spectrum slope with linear regression. In this method, the probability density function for the body size of an individual fish is

$$(3) \qquad f(x) = Cx^b, \qquad x_{\min} \leq x \leq x_{\max}$$

where

$$(4) \qquad C = \begin{cases} \dfrac{b+1}{x_{\max}^{b+1} - x_{\min}^{b+1}}, & b \neq -1 \\[3mm] \dfrac{1}{\log x_{\max} - \log x_{\min}}, & b = -1 \end{cases}$$

and x represents possible values of the body size of an individual fish, log is the natural logarithm, b is an exponent (the parameter that describes size spectrum slope, estimated via maximum likelihood), and $x_{\min}$ and $x_{\max}$ represent the minimum and maximum values of length or body mass (with $0 < x_{\min} < x_{\max}$) (Edwards et al. 2017). C is a normalization constant and is calculated by solving $\int_{x_{\min}}^{x_{\max}} f(x)dx = 1$ (Edwards et al. 2017). Accordingly, the abundance density function for a community of n individuals is

$$(5) \qquad N(x) = nf(x) = nCx^b, \qquad x_{\min} \leq x \leq x_{\max}$$

Influence of fish orientation on TS and size spectra slopes

The impact of fish orientation relative to the acoustic transducer on size spectra slopes and fish lengths can be investigated using the orientation angle of tracked fishes ("Direction_vertical" in Echoview; Echoview Software Pty.) in four ways. First, one can calculate the mean and standard deviation of orientation angle and absolute angle of all tracked fishes in each survey to determine if fishes were oriented normally to the acoustic transducer on average. Second, generalized linear models (GLMs) or generalized additive models (GAMs) can be used to examine the effect of orientation angle and absolute angle on TS. Third, the effect of average orientation angle and absolute angle on size spectra slopes can be investigated using GLMs or GAMs. Fourth, the method of de Kerckhove et al. (2016) can be employed to quantify the coefficient of variation (CV) in size spectra slopes at each site that is associated with variable estimates of TS due to variable fish orientation. This entails randomly assigning each fish a new TS value by sampling from a truncated normal distribution (truncated to the TS thresholds) with a mean equal to its observed TS and a standard deviation equal to the standard deviation of TS of all fish tracks (de Kerckhove et al. 2016). This process is iterated 1000 times for each site and the slope of the size spectrum for each of the 1000 datasets is estimated, followed by the calculation of the mean and standard deviation of slopes for each site (de Kerckhove et al. 2016).

Study area and data collection

Data for the application of our generalizable methodology were collected at 48 petroleum platforms throughout the northern US GOM over a two-year period (May through August of 2017 and 2018; Fig. 3). Forty-five of the platforms were surveyed once in a single year, and 3 of the platforms were surveyed twice (once in each year). Site visits were analyzed separately in this study. The study platforms were selected via random sampling among depth strata sensu Gallaway and Lewbel (1982). The study area and data collection procedures were described in greater detail by Bolser et al. (2020, 2021) and Egerton et al. (2021).

A Simrad EK80 split-beam echosounder with a 120 kHz transducer (circular beam width of 6.8°; pulse duration = 0.128 ms; ping rate = "max") was employed for acoustic surveys. Ping rate was set to max to achieve the highest resolution possible across the range of depths at our study sites (11–142 m). The echosounder was calibrated using a tungsten carbide sphere according to standard methods prior to each survey event (Demer et al. 2015). The transducer was deployed at a depth of 1 m using a customized mount on the starboard side of the survey vessel and aimed directly downwards. The survey track followed a spiral pattern beginning as close to the platform as possible (typically ~3 m from the legs) and ending approximately 100 m from the platform structure (Egerton et al. 2021; Bolser et al. 2021). "Passes" were separated by approximately 20 m and an additional transect was conducted perpendicular to the spiral transects on each side of the platform structure (see figure 2 in Egerton et al. 2021).

To collect data on the identity and relative abundance of fish species, a self-rotating video (SRV) drop-camera was deployed on the down-current side of the platform at 10-m depth intervals for

1260

Can. J. Fish. Aquat. Sci. Vol. 79, 2022

Fig. 3. Locations of the petroleum platforms surveyed in this study. Data from platforms where community censuses were conducted were originally presented by Gitschlag et al. (2001), base map data are from Google, and the projection used in this map is WGS 84/Pseudo-Mercator. [Colour online.]
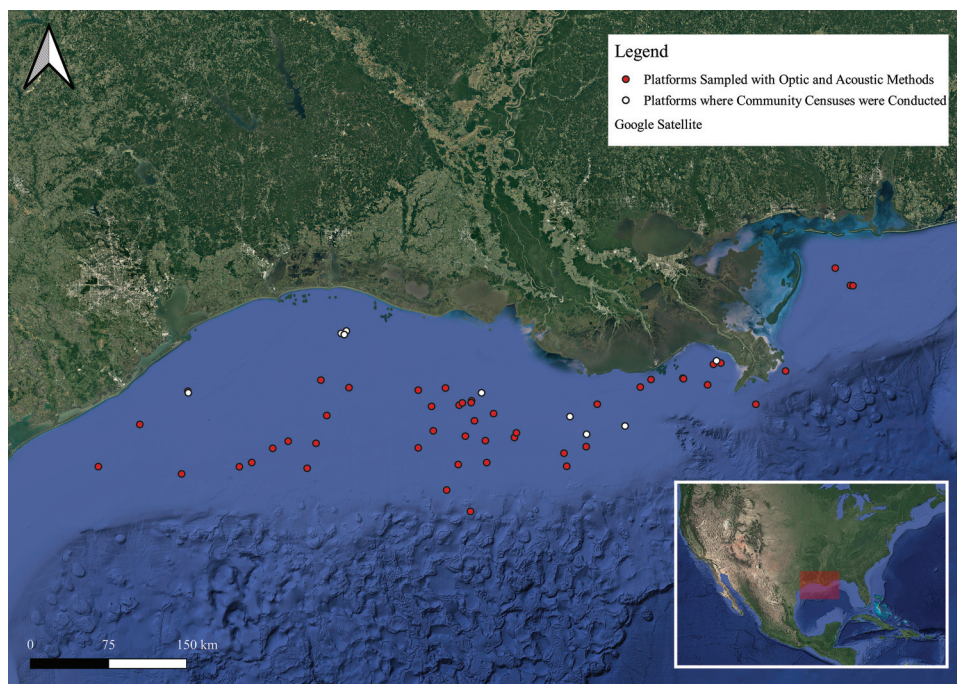
6–7 min each and at one additional location within 100 m of the study platform in the same manner if a large school of fishes was observed on the echosounder to include transient schools of pelagic fishes that were recorded by the echosounder. More details on camera sampling were reported by Bolser et al. (2020, 2021) and may be found in the online Supplementary material S7[1].

Acoustic data processing

Acoustic data were processed using Echoview software (version 10; Echoview Software Pty.) following standard procedures (Parker-Stetter 2009). The first 1–3 m of the water column (depending on sea state) were removed to account for the near-field effect of the transducer and to exclude bubbles caused by wave action (Simmonds and MacLennan 2008). Similarly, a 1-m exclusion zone was applied above the seafloor to account for the hydroacoustic dead zone near the seabed (Ona and Mitson 1996). Echograms were scrutinized to remove bubbles that penetrated deeper into the water column, electronic noise, and the platform structure. Background noise was removed using the Echoview background removal operator with a maximum noise value of 125 dB and minimum signal to noise ratio of 10 dB. TS data were thresholded at –55 dB (minimum) and –20 dB (maximum), and S_v data were thresholded based on a value of –61 dB TS_u (uncompensated target strength, minimum threshold) following Parker-Stetter (2009) and Rudstam et al. (2009) to account for off-axis detections. These thresholds were chosen to exclude most planktonic scattering sources and include most fishes, but we acknowledge that large plankton and invertebrates may not have been completely excluded.

To generate a complete representation of the fish community sampled acoustically, this analysis included tracked fishes and schools of fishes. We note that cryptobenthic fishes and fishes that were tightly associated with the platform structure likely were not sampled by the echosounder due to our conservative treatment of the seafloor and platform structure, and inherent

limitations of interpreting reverberation in rugose habitats. A fish tracking algorithm was employed within Echoview with parameters set to their defaults, and the mean TS across detections was used to define the TS of each tracked fish. Similarly, the school detection algorithm within Echoview was used to detect and delineate school shapes within the echogram with minimum total school height, minimum candidate length, minimum candidate height, and minimum total school length set to 3 m, maximum vertical linking distance set to 5 m, and maximum horizontal linking distance set to 20 m. These parameters were chosen after preliminary examinations of computing performance and school detection success. Final school detections were verified by an analyst. It was necessary to detect single targets to scale school S_v (by in situ or simulated TS, with alternate TS values estimated for each single target if scaling with simulated TS) and estimate the abundance of fishes within schools. Single targets were detected in Echoview using a pulse length determination level of 6 dB, minimum normalized pulse length of 0.7 seconds, and maximum standard deviation of 0.6 degrees for major and minor axis angles. The median number of single targets detected around schools was 48 (SD = 133, range = 1–1369).

Generation of reference datasets

To validate acoustic size spectra, it is necessary to compare them with the size spectra estimated with other methods. In rugose marine habitats such as the petroleum platforms we sampled, logistical constraints and gear biases (e.g., selectivity of hook-and-line sampling, visibility and diver avoidance for stereo video, impracticality of trawling around and over structure) limit the techniques that researchers can use to assess size spectra. Ideally, one would ensure an unbiased representation of community size structure by capturing and measuring each individual in the community or by collecting all individuals after a complete mortality event. While this was not possible at our study sites, Gitschlag et al. (2001) censused fish

---

[1]Supplementary data are available with the article at https://doi.org/10.1139/cjfas-2021-0189.

Table 2. Information about the datasets employed in this study.

Dataset name	Abbreviation	Source of abundance data	Source of length data	TS data used to scale school S_v	Type of TS–length model used
Community Census	1_Com. Cen._Avg. Len.	Field collections	Field collections	NA	NA
Simulated "expected" Community	2_Sim. Com._Avg. Len.	Acoustics	Simulations	NA	NA
General TS–length model dataset	3_in situ_Gen. TS–Len.	Acoustics	Acoustics	In situ acoustic	General
Specific TS–length model dataset	4_in situ_Spc. TS–Len.	Acoustics	Acoustics	In situ acoustic	Specific
Simulated school TS dataset — all species	5_Sim. Schl. All_Spc. TS–Len.	Acoustics	Acoustics and simulations	Simulated (all species observed)	Specific
Simulated school TS dataset — small species	6_Sim. Schl. Sm._Spc. TS–Len.	Acoustics	Acoustics and simulations	Simulated (small species)	Specific
Simulated school TS dataset — large species	7_Sim. Schl. Lg._Spc. TS–Len.	Acoustics	Acoustics and simulations	Simulated (large species)	Specific

communities after explosive decommissioning procedures at nine petroleum platforms in the GOM (Fig. 3). These procedures are typically lethal for nearly all fishes within an approximately 100 m radius of the platform (Gitschlag et al. 2001; LGL Ecological Research Associates 2019). Since fishes were collected immediately after detonation using multiple surface and underwater gears, we assumed that those fish collections accurately represented the fish communities at those decommissioned platforms. We used the data of Gitschlag et al. (2001) (hereinafter referred to as "community census" data; dataset 1, Figs. 2, 3; available from https://catalog.data.gov/dataset/fish-mortalities-from-explosive-removal-of-petroleum-platforms-in-the-gulf-of-mexico-1993-to-1999) to estimate fish community size spectra at each of their study sites as a reference to compare our acoustically derived size spectra with. We acknowledge that it is possible that the structure of fish communities at platforms may have changed since the community census data were collected but believe it to be the best available census of platform fish communities.

In addition to the community census data, we simulated an "expected" size distribution based on species composition for comparison with our acoustically derived size spectra at each of our study sites (dataset 2, Fig. 2). This simulated "expected" size distribution dataset consisted of simulated communities at each site based on the relative abundance of species from SRV camera data (as estimated using the MaxN method (Priede et al. 1994); described in detail by Bolser et al. (2020, 2021)), published biological data for each species (community census, Gitschlag et al. (2001); FishBase, Froese and Pauly (2020)), and absolute abundance of fishes derived from the acoustic data (using in situ TS data to scale school S_v to abundance). While the total abundance of fishes in this dataset was estimated with acoustics, all size and relative abundance information was estimated from non-acoustic data. Since the total number of fishes is simply a number to scale relative abundance by and size information was independent of acoustic data, we believe it was reasonable to make comparisons between results from this dataset and those derived from acoustic data.

To estimate the abundance of each species in the simulated "expected" community dataset, the total abundance of fishes at each site was multiplied by the proportional abundance of each species from SRV camera data. Lengths were then assigned to each fish of each species by randomly sampling from a truncated normal distribution (R package "truncnorm", version 1.0-8). The distribution for each species was truncated by a lower value of either the smallest fish of that species in the community census (if observed in the community census dataset) or the length at maturity from FishBase (if not observed), and an upper value of the largest fish of that species in the community census or maximum length from FishBase. The distribution was centered around either the mean length of that species in the community census or the common length from FishBase. The standard deviation of the distribution was set to the standard deviation of the length of that species from the community census, or one half of the difference

between length at maturity and maximum length from FishBase. Data for some of these parameters were not available for some species from either data source, and the alternative data used are described in the supplementary material (Supplementary Table S6.1[1]). These datasets were subsequently combined for all species observed at each site to form a complete water column fish community at each site. The basic characteristics and names of these datasets, as well as the others employed in our example, can be found in Table 2.

Generation of simulated data for abundance estimation scenarios

For the abundance estimation scenario in which single targets around schools were deemed to be composed of all species observed on SRV cameras, TS values were simulated from a truncated normal distribution centered around the mean expected TS of all species observed on SRV cameras. Expected TS was estimated by converting lengths from the community census or FishBase using specific TS–length models, which are described in detail in the subsequent section and Table 3. The distribution was truncated by a lower value of either the smallest expected TS in the community census of a species that was observed on SRV cameras or the smallest expected TS converted from the length at maturity in FishBase of species observed on SRV cameras, and an upper value of the largest expected TS in the community census of a species that was observed on SRV cameras or largest TS converted from the maximum length in FishBase of species observed on SRV cameras. The standard deviation of the distribution was set to the standard deviation of expected TS among all species observed on the SRV cameras.

The same procedure was followed to generate TS values for single targets around schools in the scenario in which TS values were simulated from those expected for small pelagic species, except that the simulation was based on the expected TS values for the following species: Atlantic bumper (*Chloroscombrus chrysurus*), Atlantic spadefish (*Chaetodipterus faber*), Bermuda chub (*Kyphosus sectatrix*), blue runner (*Caranx crysos*), and Gulf menhaden (*Brevoortia patronus*). Dense schools of fishes at our study sites were typically composed of these species (Bolser et al. 2020, 2021).

The same procedure was also followed to generate TS values for single targets around schools in the scenario in which TS values were simulated from those expected for large piscivorous species, except that the simulation was based on the expected TS values for the following species: cobia (*Rachycentron canadum*), crevalle jack (*Caranx hippos*), great barracuda (*Sphyraena barracuda*), greater amberjack (*Seriola dumerili*), horse-eye jack (*Caranx latus*), and king mackerel (*Scomberomorus cavalla*).

The basic characteristics and names of these datasets can be found in Table 2. For convenience, the datasets generated through scaling school S_v with simulated TS data are hereinafter collectively referred to as the "simulated school TS datasets" (datasets 5–7, Fig. 2). Similarly, the datasets generated using in situ TS data are hereinafter

Table 3. Specific target strength (TS) to length models used for each species.

Model (reference)	Species that the model is based on	Species that the model was applied to
TS = 53.7 log$_{10}$(length) – 130.2 (Foote 1980)	*Scomber scombrus* (Scombridae, Scombriformes)	*Scomberomorus cavalla* (Scombridae), *Sphyraena barracuda* (Scombriformes), *Sphyraena guachancho* (Scombriformes)
TS = 20 log$_{10}$(length) – 80.4 (Zhang et al. 2014)	*Epinephelus awoara* (Serranidae)	Serranidae spp. (groupers were not consistently identified to genus or species)
TS = 20 log$_{10}$(length) – 65.4 (Kang et al. 2004)	*Acanthopagrus schlegelii* (Sparidae)	*Archosargus probatocephalus* (Sparidae)
TS = 19.9 log$_{10}$(length) – 66.7 (Boswell et al. 2020)	*Balistes capriscus* (Balistidae)	*Balistes capriscus*, *Canthidermis sufflamen* (Balistidae)
TS = 20 log$_{10}$(length) – 66.65 (Hwang et al. 2015)	*Trachurus japonicus* (Caragnidae, Caragniformes)	*Carangoides bartholomaei* (Caragnidae), *Carangoides ruber* (Caragnidae), *Caranx crysos* (Caragnidae), *Caranx hippos* (Caragnidae), *Caranx latus* (Caragnidae), *Chloroscombrus chrysurus* (Caragnidae), *Elagatis bipinnulata* (Caragniformes), *Oligoplites saurus* (Caragnidae), *Rachycentron canadum* (Caragniformes), *Selene setapinnis* (Caragnidae), *Selene vomer* (Caragnidae), *Seriola dumerili* (Caragnidae), *Seriola rivoliana* (Caragnidae)
TS = 17.1 log$_{10}$(length) – 60.3 (Boswell et al. 2020)	*Lutjanus campechanus*	*Lutjanus campechanus*, *Lutjanus grisus*, *Lutjanus jocu*
TS = 18.2 log$_{10}$(length) – 65.8 (Boswell et al. 2020)	*Haemulon aurolineatum* (Haemulidae, Perciformes)	*Chaetodipterus faber* (Perciformes), *Kyphosus sectatrix* (Perciformes), *Pomatomus saltatrix* (Perciformes), *Scianops ocellatus* (Perciformes)
TS = 18.8 log$_{10}$(length) – 62.4 (Nakken and Olsen 1977)	*Clupea harengus* (Clupeidae)	*Brevoortia patronus* (Clupeidae)
TS = 51.7 log$_{10}$(length) – 118.6 (Boswell et al. 2020)	*Rhomboplites aurorubens*	*Rhomboplites aurorubens*

Note: Family and order names are included to show the relatedness of each observed species to the species on which the model was based.

collectively referred to as the "in situ school TS datasets" (datasets 3 and 4, Fig. 2).

Specific target strength–length models used

A species-specific model was not available for all of the 29 species included in this study, so models for related species were used (same species: 3 of 29; same genus: 5 of 29; same family: 21 of 29; same order: 29 of 29; Table 3). For assigning a species identity to each TS observation, we converted mean length in the community census (if the species was represented) or "common length" from FishBase (if the species was not represented in the community census data) of each species to TS using the closest published TS–length formula for the observed species and proceeded with the procedure described in the "Conversion of TS to length" section. The dataset resulting from the application of this procedure to the in situ school TS dataset is hereinafter referred to as the "Specific TS–length model dataset" (dataset 4, Fig. 2). In contrast, the dataset resulting from the application of the Love (1971) model is hereinafter referred to as the "General TS–length model dataset" (dataset 3, Fig. 2). TS was converted to length using specific TS–length models for each of the simulated school TS datasets (5–7, Fig. 2).

Orientation analysis

We used Gamma GLMs with inverse link functions to examine the effect of orientation angle and absolute angle on TS in our example (base "stats" R package, version 3.6.1). We investigated the effect of average orientation angle and absolute angle on size spectra slopes using Gamma GLMs with log link functions (base "stats" R package, version 3.6.1). These models were fit to the absolute value of slope to facilitate the use of log link functions, which, after preliminary examination of data properties, were deemed to be most appropriate for these datasets. GAMs were also explored for the second and third analyses, but their fits were nearly identical to GLM fits, so GLMs were chosen for parsimony. We conducted the simulation analysis of de Kerckhove et al. (2016), which was designed to quantify the effect of variation in TS (due to variation in the orientation of fishes), on size spectra slopes on the in situ school TS datasets (3 and 4, Fig. 2).

Statistical comparisons of size spectra slopes and mean length of fishes between datasets

Nonparametric Kruskal–Wallis (KW) tests with Dunn's multiple comparison post hoc tests were used to determine significant differences between size spectrum slopes generated from each dataset in R Studio (Kruskal–Wallis test: base "stats" package, version 3.6.1; Dunn's post hoc test: "FSA" package, version 0.8.31; Ogle et al. 2020). The same procedure was used to compare the median length of fishes in each dataset.

Statistical comparisons were also conducted on all datasets except for the community census after they were filtered to include only surveys with good water clarity for ground-truthing (SRV camera visibility score of >2.0 out of 3.0; see Bolser et al. (2020) for scoring details) and a mean fish orientation angle (from tracked fishes; see below) within 2.0° of normal to the horizontal axis. The visibility threshold for SRV camera data was chosen based on the analyses of Bolser et al. (2021), who linked SRV camera and acoustic data and examined biases in a dataset containing the study platforms. The threshold for orientation was chosen as a relatively conservative level that removed outlying slopes based on preliminary examination of the data. These analyses were also conducted for data thresholded by visibility alone and orientation angle alone. Mann–Whitney–Wilcoxon rank sum tests were used to compare slopes and fish lengths between each type of full and reduced datasets in R Studio (base "stats" R package, version 3.6.1).

Results

Summary of species observed

A total of 29 species were observed by SRV cameras at our study sites and considered in this analysis (listed in Table 3). We observed 11 additional species but excluded them from the analysis as they were unlikely to be detected by the echosounder due to their close association with the platform structure or exceptionally low relative abundance (Bolser et al. 2021; Supplementary Table S7.1[1]). The median Shannon–Wiener diversity at our study sites was 2.08 (range: 0–2.71) and the median species richness was 8 (range: 1–15).

Fig. 4. Boxplots of fish length. Letters indicate similar and different groups based on Dunn's Kruskal–Wallis multiple comparison post hoc test. See Table 2 for details on each dataset.
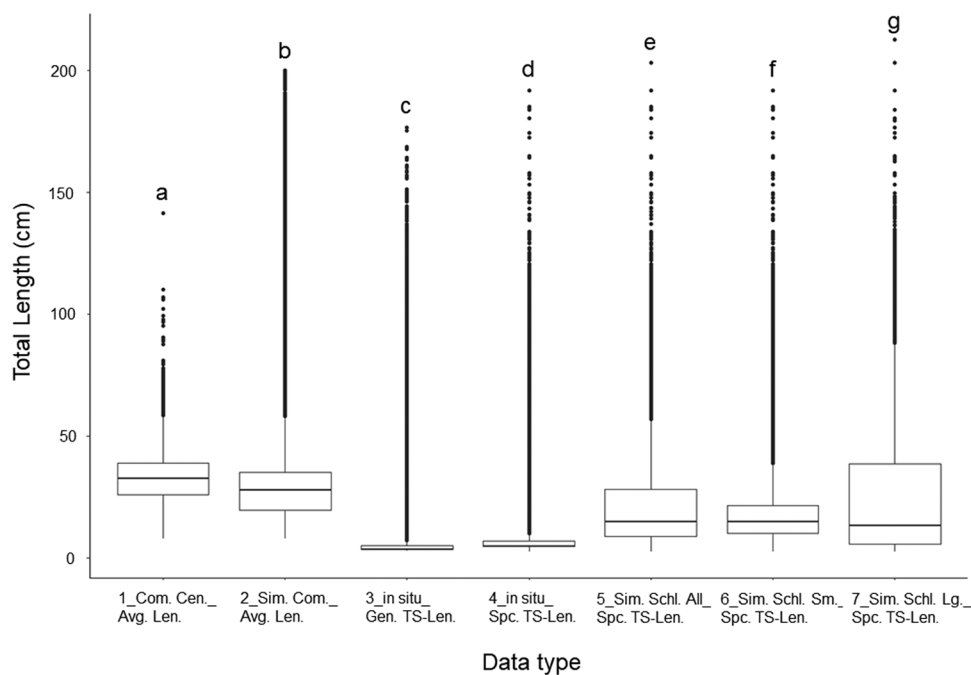
Table 4. Median (standard deviation in parentheses) fish length (cm) and size spectrum slope in each dataset.

	Community census	Simulated "expected" community	Specific TS–length model dataset	General TS–length model dataset	Simulated school TS dataset		
					All species	Small species	Large species
Fish length (cm)	32.50 (10.83)	27.87 (15.71)	4.74 (6.03)	3.48 (4.67)	14.80 (16.59)	14.80 (9.79)	13.30 (33.02)
Size spectrum slope	−1.20 (0.53)	−1.29 (0.90)	−2.59 (1.12)	−2.33 (0.88)	−1.38 (0.48)	−1.48 (0.45)	−1.24 (0.57)

Note: See Table 2 for details on each dataset.

Comparison of fish lengths

The KW test revealed that median fish lengths in all datasets were significantly different from one another (KW χ^2 = 7 107 693, $p < 0.0001$, df = 6; Fig. 4; Supplementary Table S1.6[1]). The Dunn's post hoc test showed that median fish lengths from the community census (dataset 1, Fig. 2) and simulated "expected" communities (dataset 2, Fig. 2) were longer than lengths derived from acoustics (datasets 3–7, Fig. 2), particularly in the in situ TS datasets (3 and 4, Fig. 2), regardless of the type of TS–length model used (Fig. 2; Table 4; Supplementary Table S1.6[1]). Differences between median fish lengths in each simulated scenario for single targets around schools (datasets 5–7, Fig. 2) were small, though statistically significant (Fig. 4; Table 4; Supplementary Table S1.6[1]).

Comparison of size spectra slopes

The KW test showed that there were significant differences in size spectra slopes between datasets (KW χ^2 = 118.85, $p < 0.0001$, df = 3; Fig. 5; Supplementary Table S1.5[1]), with slopes from the in situ school TS datasets (3 and 4, Fig. 1) being significantly steeper than slopes derived from the other datasets based on Dunn's post hoc test results (Fig. 5; Table 4; Supplementary Table S1.5[1]). Slopes from the community census (dataset 1, Fig. 2), simulated "expected" community (dataset 2, Fig. 2), and simulated school TS datasets (5–7, Fig. 2) were not significantly different from one another based on Dunn's post hoc test results (Fig. 5; Supplementary Table S1.5[1]).

Comparisons of fish lengths and size spectra slopes in data filtered for water clarity and mean orientation

Results of Mann–Whitney–Wilcoxon rank sum tests comparing median fish lengths and size spectra slopes in datasets that were filtered for water clarity and mean orientation are presented in the Supplementary information[1], as are the length and slope values themselves (Supplementary material S2-5[1]). Briefly, excluding surveys with unsuitable water clarity for ground-truthing or mean orientations of >2° and <−2° did not result in conclusions that differed from those drawn from the full datasets.

Influence of fish orientation on TS and size spectra slopes

While fishes were generally oriented normally to the horizontal axis (mean = 0.3°, N = 118 551), there was considerable variation (SD = 15.6°). The mean absolute value of orientation angle for all tracked fishes was 10.4° (SD = 11.6°). Despite significant p values, the low adjusted-R^2 values of Gamma GLMs indicated that orientation angle (adj. R^2 = 3.47e^{-5}, $p < 0.01$) and the absolute value of orientation angle (adj. R^2 = 2.87e^{-3}, $p < 0.001$) were not suitable predictors of TS in our data. Mean orientation angle did not have a significant effect on size spectra slopes in the Gamma GLM fit to the specific TS–length model dataset (dataset 4, Fig. 2; adj. R^2 = 0.01, $p = 0.20$) or in the Gamma GLM fit to the general TS–length model dataset (dataset 3, Fig. 2; adj. R^2 = 0.03, $p = 0.09$). Similarly, mean absolute orientation angle did not have a significant effect on size spectrum slope in the Gamma GLM fit to the specific TS–length model dataset (dataset 4, Fig. 2; adj. R^2 = 0.01, $p = 0.06$) or in the Gamma GLM fit to the general TS–length model dataset

1264

Can. J. Fish. Aquat. Sci. Vol. 79, 2022

Fig. 5. Boxplots of size spectrum slopes. Letters indicate similar and different groups based on Dunn's Kruskal–Wallis multiple comparison post hoc test. See Table 2 for details on each dataset.
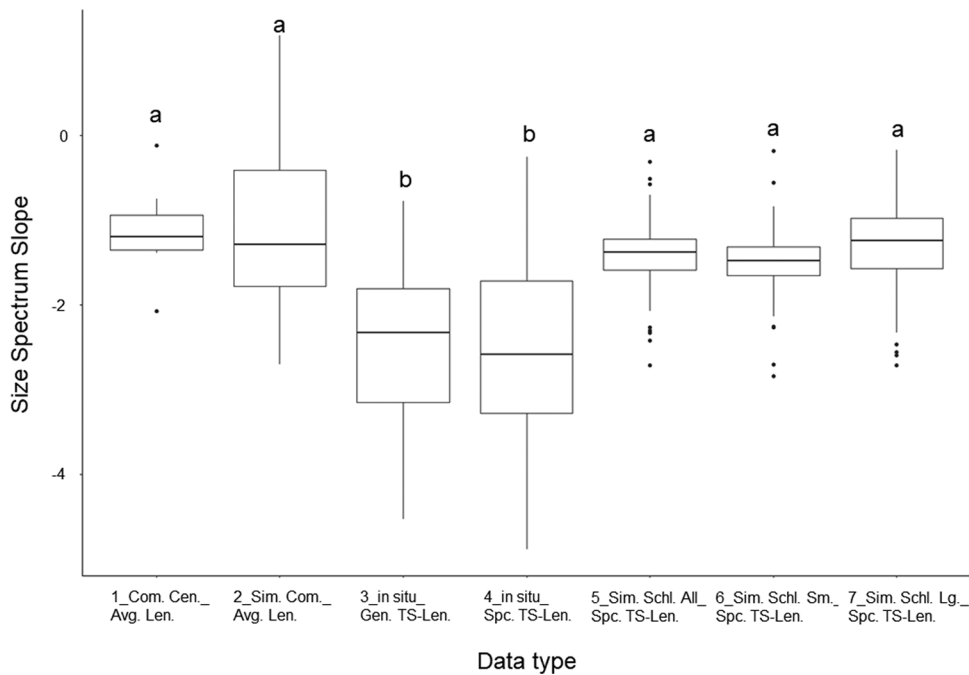
(dataset 3, Fig. 2; adj. R^2 = 0.01, p = 0.10). In the simulations designed to assess the influence of TS variation due to variable fish orientation on size spectra slopes, the average CV of TS variation on size spectrum slope was 0.7% in the general TS–length dataset (dataset 3, Fig. 1) and 0.8% in the specific TS–length dataset (dataset 4, Fig. 2; Supplementary Table S1.4[1]).

Discussion

Assessing the size spectra of marine fish communities involves numerous challenges related to the conversion of TS to length, assigning a species identity to TS observations, and attributing taxa-level information when scaling the S_v of schools to fish density and abundance. Here, we presented generalizable methodology that can be applied in a variety of situations to examine the impact of those challenges on acoustic size spectra. Using this approach can inform the degree to which acoustic size spectra may be comparable to size spectra generated from non-acoustic data and aid in identifying the source of discrepancies between acoustic and non-acoustic results.

In our example for data collected at GOM petroleum platforms, we found that fish lengths were underestimated in all acoustic datasets compared to censused communities at petroleum platforms (dataset 1, Fig. 2) and simulated "expected" communities (dataset 2, Fig. 2) at our study sites (Fig. 3). However, size spectra slopes derived from the simulated school TS datasets (5–7, Fig. 2) were comparable to those derived from reference datasets (1 and 2, Fig. 2; Fig. 5). This was the case regardless of whether specific or general models were used to convert TS to length. We did not find that fish orientation was a suitable predictor of TS or size spectra slope, although the effect of orientation on TS likely explains why slopes derived from the in situ school TS datasets (3 and 4, Fig. 2) were not comparable with those derived from reference datasets (1 and 2, Fig. 2), while slopes derived from the simulated school TS datasets (5–7, Fig. 2) were.

There is a large body of literature documenting the influence of orientation angle on TS, and thus estimated fish length, for individuals of a single species (e.g., Nakken and Olsen 1977;

McClatchie et al. 1996b; Simmonds and MacLennan 2008). The effect of orientation on in situ TS in mixed species assemblages has received less attention but could be an important source of uncertainty in acoustic size spectra studies. We did not find that orientation or absolute orientation were suitable predictors of size spectra slopes or TS in GLMs fit to our data, and CVs in simulations designed to assess the effects of orientation on size spectra slopes were low. Our explanation of this finding is that the effect of fish length and swim bladder presence or absence on TS was likely larger than the effect of orientation on TS in the diverse communities we sampled when considered as a whole. However, many in situ TS measurements for single targets around schools were smaller than predicted based on the expected TS of the species observed — even in the simulated scenario in which single targets around schools comprised only small pelagic fishes. Thus, the mean and median of in situ TS distributions around schools were smaller than in any simulated scenario. Considering the relatively small sample sizes of single targets around schools (median = 48, SD = 133, range = 1–1369), it is likely that these discrepancies were due to fishes around schools having orientations that were not normal to the horizontal axis or being disproportionately small individuals, potentially of species without swim bladders. Using TS measurements from fishes at increased distances away from the school — thus increasing the number of single targets used to represent TS of fishes in the school — could reduce the likelihood that single target TS would be biased by extreme orientation (i.e., orientation far from normal to the horizontal axis) or disproportionally small. However, this would cause size spectra slope estimates to converge on those derived from tracked fishes alone (i.e., non-schooling fishes).

The influence of single target TS distributions around schools on size spectra slopes are exacerbated when they are used to scale the S_v of schools to fish density and abundance. Consider this scenario: in the in situ school TS datasets (3 and 4, Fig. 2), the TS of fish around schools is underestimated due to extreme orientations and used for computing school density, causing density — and subsequently abundance — to be overestimated. Our procedure would magnify the effect of underestimating the TS of fishes

around schools on size spectra slopes, as the many fishes within schools would be assigned the underestimated TS values, causing fish lengths to be underestimated. Accordingly, TS estimates for single targets around schools have a disproportionate effect on size spectra slopes, as they ultimately affect both the estimated number and length of fishes within schools. Estimating comparatively larger numbers of small organisms in a community results in steeper size spectra slopes (Bianchi et al. 2000; Daan et al. 2005; Sweeting et al. 2009), as was observed when the in situ school TS datasets (3 and 4, Fig. 2) were compared with other datasets (Fig. 3; Table 4). Thus, we believe that underestimation of the TS and (or) length of single targets around schools explains the difference between results derived from in situ TS data and those derived from other acoustic datasets.

Scaling school S_v with in situ or simulated TS data involves making significant assumptions about the degree to which those data represent the TS of fishes within schools. It was not possible to directly test the validity of those assumptions by measuring the lengths of fishes in the present study, but our three simulations for the TS distribution of single targets around schools (datasets 5–7, Fig. 2) were designed to represent three possible scenarios based on our species compositions and fish behavior. Comparing data from these scenarios therefore facilitates inferences on the degree to which species composition around schools affects size spectrum slopes and fish lengths. Size spectra slopes and fish lengths estimated in each of the scenarios were similar to one another (though fish lengths were statistically different, likely due to large sample sizes; Fig. 4; Table 4; Supplementary Tables S1.6, S8.1[1]), and each scenario produced size spectra slopes that were comparable to those derived from reference datasets (1 and 2, Fig. 2). This contrasts with the in situ school TS datasets (3 and 4, Fig. 2), which exhibited size spectra slopes that were significantly steeper than all other datasets — possibly due to the effect of fishes around schools not being normally oriented to the horizontal axis or being disproportionately small, as discussed above. Based on SRV camera observations, we believe that it is more likely that these individuals were oriented at extreme angles than being disproportionately small, so we propose that the orientation of fishes around schools may be more impactful than their species identity on size spectra slopes when using their TS to scale school S_v and generate size distributions.

Fish lengths were shorter in acoustic datasets (3–7, Fig. 2) than in reference datasets (1 and 2, Fig. 2), even when the TS of single targets around schools was simulated (datasets 5–7, Fig. 2). A possible explanation for this is the presence of large numbers of swim-bladder-less fishes in the communities we sampled (Bolser et al. 2020, 2021). Swim-bladder-less fishes (e.g., carangids) have significantly weaker TS than fishes of a similar size with a swim bladder (Foote 1980; McClatchie et al. 1996a; Simmonds and MacLennan 2008). While we did not estimate the length of a swim-bladder-less fish with a model based on a fish with a swim bladder, and vice-versa, lengths often differed between the species that the model was developed for and the species that we applied the model to. Further, the comparability of the general TS–length model of Love (1971) and other TS–length models or measured lengths for fishes with swim bladders varies depending on size class and species (e.g., Fleischer et al. 1997; Mehner 2006; Wanzenböck et al. 2020). Size spectra slopes and fish lengths derived from the general TS–length model of Love (1971) and the specific TS–length models we employed were similar, but clearly, more work must be done to develop specific TS–length models for more species in our study area (e.g., Boswell et al. 2020), as each species did not have its own specific model. Species-specific models that are designed to incorporate the effect of orientation angle on TS would be particularly desirable and would help definitively identify the source of discrepancies in fish length between acoustics and other methods in size spectra studies.

Our procedure for applying specific TS–length models involved some nontrivial assumptions. We assigned a species identity to TS observations by sorting TS from smallest to largest and species from smallest to largest based on their expected TS. As identified above, the TS of a small-bladdered fish could overlap with the TS of a larger swim-bladder-less fish. If this occurred, an incorrect TS–length model could have been applied, which could substantially affect length estimates. Possible examples of this occurring may be found in the outlying points in Fig. 4. Considering that size spectra slopes were comparable within the simulated school TS datasets (5–7, Fig. 2), we propose that discrepancies in fish lengths between acoustic datasets (3–7, Fig. 2) and reference datasets (1 and 2, Fig. 2) were most likely due to the TS–length models systematically underestimating the length of individuals in all size classes. Swim-bladder-less fishes were found in nearly all size classes at our study sites, and if their lengths were consistently underestimated, it is possible that median length could be significantly shorter in acoustic datasets (3–7, Fig. 2) than in reference datasets (1 and 2, Fig. 2), while size spectra slopes were comparable.

To fully validate acoustic size spectra, they must be directly compared with data derived from other methods applied at the same time and place. This was not possible in our study given the numerous logistical constraints associated with surveying fish communities at marine petroleum platforms. However, the community census data (dataset 1, Fig. 2) provided a useful reference for platform fish community size distribution that was likely free of significant gear bias. We note that it is possible that fish communities at platforms have changed in the ∼20 years since the community census was conducted, particularly given the high fishing pressure petroleum platforms experience (Schuett et al. 2016; Cowan and Rose 2016; Stunz and Coffey 2020), which alters size structure of fish communities by making larger fishes less represented (Mason 1998; Jennings and Kaiser 1998; Berkeley et al. 2004). This would result in steeper size spectra slopes (Pope and Knights 1982; Blanchard et al. 2009; Robinson et al. 2017), as we observed in the in situ school TS datasets (3 and 4, Fig. 2) relative to others. On the other hand, the populations of some abundant platform-associated species have undergone significant rebuilding over the last ∼20 years in the GOM (e.g., red snapper (*Lutjanus campechanus*), SEDAR 2018; vermilion snapper (*Rhomboplites aurorubens*), SEDAR 2020), which might act to flatten (i.e., make less negative) size spectra slopes. It is also possible that size distributions among platforms varied throughout our study area, confounding the comparison of our data with the community census data, which were collected over a relatively narrow spatial range. Indeed, Egerton et al. (2021) reported spatial differences in the mean TS of fishes surrounding GOM petroleum platforms, which were associated with variation in salinity and temperature between study sites. Given that size information was taken from community census data for many species, spatial variability in size compositions between platforms and changes in the size of fishes at platforms over the past ∼20 years would have a large influence on the results of the present study. Size information was taken from community census data for 40% of species in our simulated "expected" community dataset (dataset 2, Fig. 2) and informed the TS simulations in the simulated school TS datasets (5–7, Fig. 2) for between 0%–80% of species depending on the scenario (although all species were not observed at every site, so percentages ranged from 0%–100% on a site-by-site basis).

The results of prior studies validating the measurement of size spectra with acoustics in freshwater environments through comparisons with other gears have been inconclusive when considered as a whole (Coll et al. 2007; de Kerckhove et al. 2016; Daigle 2017). We were unable to find direct comparisons of size spectra slopes between acoustics and other gears in the literature, although size distributions may be reasonably comparable between acoustics and netting approaches in some cases, depending on selectivity, sampling locations, and treatment of tracked fish TS (Coll et al. 2007;

1266

Can. J. Fish. Aquat. Sci. Vol. 79, 2022

de Kerckhove et al. 2016; Daigle 2017). Acoustically derived lengths have been shown to be shorter than those estimated by netting (Coll et al. 2007; Daigle 2017) and fishery data (Coll et al. 2007), although it is difficult to identify actual discrepancies from the effects of selectivity in these studies. Our finding that acoustic sampling underestimates the length of fishes compared to our reference datasets (1 and 2, Fig. 2) agrees with prior findings (Coll et al. 2007; Daigle 2017), potentially suggesting that selectivity may not have been a major determinant of their results. However, those studies employed the general TS–length model of Love (1971). Thus, it is possible that the acoustic results could have changed if specific TS–length models were applied.

The size spectra slopes we estimated with acoustics around marine petroleum platforms were generally less steep than size spectra slopes estimated with acoustics in lakes (Wheeland and Rose 2016; de Kerckhove et al. 2016; Daigle 2017; range of cited studies: 9.22 to –0.4) and steeper than slopes estimated with acoustics in other types of structurally complex marine habitats (Egerton 2017; –0.38 to –0.03). We note, however, that the size spectra reported by Egerton (2017) exhibited domes, which complicates interpretation of slopes. Studies that assessed marine fish size spectra in structurally complex marine habitats employing non-acoustic methods generally showed slopes that were less steep or similar to those derived from acoustic data in the present study (e.g., Graham et al. 2005, 2007; McClanahan and Graham 2005; Wilson et al. 2010; Robinson et al. 2017; range of cited studies: –1.95 to –0.03). While it is difficult to make quantitative comparisons between our results and other studies because of methodological differences (e.g., method of calculating slope; Robinson and Baum 2016; Edwards et al. 2017), our results were more similar to studies in similar habitats using different gears than they were to studies in different habitats using acoustics.

Despite favorable comparisons between size spectra slopes in the simulated school TS datasets (5–7, Fig. 2) with reference datasets (1 and 2, Fig. 2), it is clear that more research is needed before acoustic data are used to make ecological inferences about marine fish communities such as those we sampled at petroleum platforms. Future work should extend validation efforts to direct comparisons between different gear types in marine environments (e.g., stereo cameras, acoustics, direct capture), as has been done in freshwater systems (Coll et al. 2007; de Kerckhove et al. 2016; Daigle 2017). These validation efforts will be useful for determining the degree to which the discrepancies we observed were due to assumptions and uncertainty associated with using acoustic data to assess the size spectra of fish communities, or actual differences in communities over time and space. Stereo cameras would be especially attractive for comparisons with acoustics in environments such as the marine petroleum platforms we sampled, as they could be easily deployed in the same manner as the SRV cameras we used in the present study. However, it would be ideal if future studies could fully co-reference acoustic and ground-truthing data (i.e., simultaneously collect optic and acoustic data for each fish). We did not have co-referenced optic and acoustic data, and while the SRV cameras recorded water column fishes around the platform structure and a separate "targeted drop" was conducted away from the platform if a large school was observed on the echosounder, it is possible that the SRV camera data did not completely represent the assemblage of water column fishes sampled by acoustics. Along with direct comparisons with non-acoustic data and the development of TS–length models for additional species that incorporate orientation, future work should investigate the potential for assigning a species identity to fish within schools based on school characteristics (e.g., Horne 2000; Simonsen 2013; Campanella and Taylor 2016) and otherwise determining the optimal source of TS data for scaling school S_v. Given the discrepancies between size spectra slopes and fish lengths derived from using in situ and simulated TS data around schools to scale school S_v, developing robust methods for assigning TS and taxonomic information to schools is paramount to operationalizing acoustic size spectra metrics for ecological inferences. We view further research effort in these areas as worthwhile considering how rapidly acoustic data can be collected, which would make acoustic size spectra slopes efficient indicators that could be assessed frequently over large spatial and temporal scales.

Although assessing size spectra with acoustics in marine habitats where large numbers of swim-bladder-less and schooling fishes are found (e.g., reef habitats) presents numerous challenges relative to other situations, it is important to monitor communities in these areas as they are often affected by a variety of natural and anthropogenic stressors and can support economically important fisheries. The fish communities at petroleum platforms in the GOM that we studied in our example vary seasonally (Stanley and Wilson 1997; Barker and Cowan 2018; Reynolds et al. 2018) and are affected by numerous environmental variables, particularly those related to freshwater inflow and circulation patterns (Gallaway and Lewbel 1982; Munnelly et al. 2021; Bolser et al. 2021). They are also are subject to high levels of fishing pressure (Schuett et al. 2016; Cowan and Rose 2016; Stunz and Coffey 2020) and have been increasingly affected by decommissioning procedures, resulting in a net decrease in platform habitat over the last decade (Gitschlag et al. 2001; LGL Ecological Research Associates 2019; Munnelly et al. 2021). Assessing the size spectra of marine fish communities with acoustics at platforms and similar habitats would allow the effects of these influences on community structure to be efficiently summarized in a standardized manner, allowing for powerful spatiotemporal comparisons.

Conclusion

We developed an approach for quantitatively assessing the challenges associated with estimating fish community size spectra with hydroacoustics in marine environments. These challenges are perhaps most pronounced in marine reef habitats but can be found in anywhere, so our approach could be replicated in any system to gain insights on the influence of common assumptions, sources of bias, and uncertainty in acoustic size spectra studies. In our GOM example, the source of TS data used to scale the S_v of schools of fishes to abundance had a greater influence on size spectra slopes than fish orientation or TS–length model choice. Accordingly, future acoustic size spectra research should focus on examining school characteristics and the behavior of fishes adjacent to schools to better assign taxonomic and TS information to schools. We recommend direct comparisons between acoustic size spectra and size spectra derived through other means (e.g., stereo cameras, direct capture) and similar examinations of the differential impacts of fish orientation, TS–length model choice, and source of school TS information in other marine systems. At present, we caution drawing ecological inferences from acoustic size spectra metrics in systems such as the marine petroleum platforms we studied. In the future, however, our results suggest that size spectra metrics may be suitable for ecological inferences if TS and taxonomic information can be more robustly attributed to schools and direct comparisons between acoustic and non-acoustic data are made across different systems.

Acknowledgements

References

Andersen, K.H., Jacobsen, N.S., and Farnsworth, K.D. 2016. The theoretical foundations for size spectrum models of fish communities. Can. J. Fish. Aquat. Sci. **73**(4): 575–588. doi:10.1139/cjfas-2015-0230.

Barker, V.A., and Cowan, J.H. 2018. The effect of artificial light on the community structure of reef-associated fishes at oil and gas platforms in the northern Gulf of Mexico. Environ. Biol. Fishes, **101**(1): 153–166. doi:10.1007/s10641-017-0688-9.

Benoit-Bird, K.J., Au, W.W.L., and Kelley, C.D. 2003. Acoustic backscattering by Hawaiian lutjanid snappers. I. Target strength and swimbladder characteristics. J. Acoust. Soc. Am. **114**(5): 2757–2766. doi:10.1121/1.1614256. PMID:14650010.

Berkeley, S.A., Hixon, M.A., Larson, R.J., and Love, M.S. 2004. Fisheries sustainability via protection of age structure and spatial distribution of fish populations. Fisheries, **29**(8): 23–32. doi:10.1577/1548-8446(2004)29[23:FSVPOA]2.0.CO;2.

Bianchi, G., Gislason, H., Graham, K., Hill, L., Jin, X., Koranteng, K., et al. 2000. Impact of fishing on size composition and diversity of demersal fish communities. ICES J. Mar. Sci. **57**(3): 558–571. doi:10.1006/jmsc.2000.0727.

Blanchard, J.L., Jennings, S., Law, R., Castle, M.D., McCloghrie, P., Rochet, M.-J., and Benoît, E. 2009. How does abundance scale with body size in coupled size-structured food webs? J. Anim. Ecol. **78**(1): 270–280. doi:10.1111/j.1365-2656.2008.01466.x. PMID:19120607.

Blanchard, J.L., Heneghan, R.F., Everett, J.D., Trebilco, R., and Richardson, A.J. 2017. From bacteria to whales: using functional size spectra to model marine ecosystems. Trends Ecol. Evol. **32**(3): 174–186. doi:10.1016/j.tree.2016.12.003. PMID:28109686.

Bolser, D.G., Egerton, J.P., Grüss, A., Loughran, T., Beyea, T., McCain, K., and Erisman, B.E. 2020. Environmental and structural drivers of fish distributions among petroleum platforms across the U.S. Gulf of Mexico. Mar. Coast. Fish. **12**(2): 142–163. doi:10.1002/mcf2.10116.

Bolser, D.G., Egerton, J.P., Grüss, A., and Erisman, B.E. 2021. Optic-acoustic analysis of fish assemblages at petroleum platforms. Fisheries, **46**(11): 552–563. doi:10.1002/fsh.10654.

Boswell, K.M., Wells, R.J., Cowan, J.H., Jr., and Wilson, C.A. 2010. Biomass, density, and size distributions of fishes associated with a large-scale artificial reef complex in the Gulf of Mexico. Bull. Mar. Sci. **86**(4): 879–889. doi:10.5343/bms.2010.1026.

Boswell, K.M., Pedersen, G., Taylor, J.C., LaBua, S., and Patterson, W.F. 2020. Examining the relationship between morphological variation and modeled broadband scattering responses of reef-associated fishes from the southeast United States. Fish. Res. **228**: 105590. doi:10.1016/j.fishres.2020.105590.

Campanella, F., and Taylor, J.C. 2016. Investigating acoustic diversity of fish aggregations in coral reef ecosystems from multifrequency fishery sonar surveys. Fish. Res. **181**: 63–76. doi:10.1016/j.fishres.2016.03.027.

Coll, C., Morais, L.T., de, , Laë, R., Lebourges-Dhaussy, A., Simier, M., Guillard, J., et al. 2007. Use and limits of three methods for assessing fish size spectra and fish abundance in two tropical man-made lakes. Fish. Res. **83**(2): 306–318. doi:10.1016/j.fishres.2006.10.005.

Cowan, J.H., and Rose, K.A. 2016. Oil and gas platforms in the Gulf of Mexico: their relationship to fish and fisheries. In Fisheries and aquaculture in the modern world. IntechOpen. doi:10.5772/63026.

Daan, N., Gislason, H., Pope, J.G., and Rice, J.C. 2005. Changes in the North Sea fish community: evidence of indirect effects of fishing? ICES J. Mar. Sci. **62**(2): 177–188. doi:10.1016/j.icesjms.2004.08.020.

Daigle, A.A. 2017. Hydroacoustic assessment of fish community size spectra refinement of hydroacoustic estimates of size. Thesis. Available from https://tspace.library.utoronto.ca/handle/1807/79235 [accessed 18 September 2019].

de Blois, S. 2020. The 2019 Joint U.S.–Canada Integrated Ecosystem and Pacific Hake Acoustic-Trawl Survey: Cruise Report SH-19-06. US Department of Commerce, NOAA Processed Report NMFS-NWFSC-PR-2020-03.

de Kerckhove, D.T., Shuter, B.J., and Milne, S. 2016. Acoustically derived fish size spectra within a lake and the statistical power to detect environmental change. Can. J. Fish. Aquat. Sci. **73**(4): 565–574. doi:10.1139/cjfas-2015-0222.

Demer, D.A., Berger, L., Bernasconi, M., Bethke, E., Boswell, K., Chu, D., et al. 2015. Calibration of acoustic instruments. Report, International Council for the Exploration of the Sea (ICES). doi:10.25607/OBP-185.

Edwards, A.M., Robinson, J.P.W., Plank, M.J., Baum, J.K., and Blanchard, J.L. 2017. Testing and recommending methods for fitting size spectra to data. Methods Ecol. Evol. **8**(1): 57–67. doi:10.1111/2041-210X.12641.

Egerton, J.P. 2017. Hydroacoustics as a tool for the assessment of fishes within existing and candidate marine protected areas (MPAs). Ph.D. thesis, Bangor University, Wales, United Kingdom. Available from https://search.proquest.com/docview/2083744682/abstract/47C3122F78CB43BBPQ/1 [accessed 24 November 2020].

Egerton, J.P., Bolser, D.G., Grüss, A., and Erisman, B.E. 2021. Understanding patterns of fish backscatter, size and density around petroleum platforms of the U.S. Gulf of Mexico using hydroacoustic data. Fish. Res. **233**: 105752. doi:10.1016/j.fishres.2020.105752.

Elton, C. 1946. Competition and the structure of ecological communities. J. Anim. Ecol. **15**(1): 54–68. doi:10.2307/1625.

Emmrich, M., Brucet, S., Ritterbusch, D., and Mehner, T. 2011. Size spectra of lake fish assemblages: responses along gradients of general environmental factors and intensity of lake-use. Freshw. Biol. **56**(11): 2316–2333. doi:10.1111/j.1365-2427.2011.02658.x.

Fleischer, G.W., Argyle, R.L., and Curtis, G.L. 1997. In situ relations of target strength to fish size for Great Lakes pelagic planktivores. Trans. Am. Fish. Soc. **126**(5): 786–794. doi:10.1577/1548-8659(1997)126<0786:ISROTS>2.3.CO;2.

Foote, K.G. 1979. On representing the length dependence of acoustic target strengths of fish. J. Fish. Res. Board Can. **36**(12): 1490–1496. doi:10.1139/f79-216.

Foote, K.G. 1980. Importance of the swimbladder in acoustic scattering by fish: A comparison of gadoid and mackerel target strengths. J. Acoust. Soc. Am. **67**(6): 2084–2089. doi:10.1121/1.384452.

Froese, R., and Pauly, D. 2020. FishBase. World Wide Web electronic publication, version (12/2019).

Gallaway, B.J., and Lewbel, G.S. 1982. The ecology of petroleum platforms in the northwestern Gulf of Mexico: A Community Profile. US Department of the Interior, Bureau of Land Management, Fish and Wildlife Service.

Gitschlag, G.R., Schirripa, M.J., and Powers, J.E. 2001. Estimation of fisheries impacts due to underwater explosives used to sever and salvage oil and gas platforms in the U.S. Gulf of Mexico. United States Department of the Interior. Available from https://digital.library.unt.edu/ark:/67531/metadc955391/ [accessed 23 November 2020].

Graham, N.A.J., Dulvy, N.K., Jennings, S., and Polunin, N.V.C. 2005. Size-spectra as indicators of the effects of fishing on coral reef fish assemblages. Coral Reefs, **24**(1): 118–124. doi:10.1007/s00338-004-0466-y.

Graham, N.A.J., Wilson, S.K., Jennings, S., Polunin, N.V.C., Robinson, J., Bijoux, J.P., and Daw, T.M. 2007. Lag effects in the impacts of mass coral bleaching on coral reef fish, fisheries, and ecosystems. Conserv. Biol. **21**(5): 1291–1300. doi:10.1111/j.1523-1739.2007.00754.x. PMID:17883494.

Heneghan, R.F., Hatton, I.A., and Galbraith, E.D. 2019. Climate change impacts on marine ecosystems through the lens of the size spectrum. Emerg. Top. Life Sci. **3**(2): 233–243. doi:10.1042/ETLS20190042. PMID:33523153.

Horne, J.K. 2000. Acoustic approaches to remote species identification: a review. Fish. Oceanogr. **9**(4): 356–371. doi:10.1046/j.1365-2419.2000.00143.x.

Hwang, K., Yoon, E.A., Lee, K., Lee, H., and Hwang, D.J. 2015. Multifrequency acoustic scattering characteristics of jack mackerel by KRM model. J. Korean Soc. Fish. Technol. **51**(3): 424–431. doi:10.3796/KSFT.2015.51.3.424.

Jennings, S., and Dulvy, N.K. 2005. Reference points and reference directions for size-based indicators of community structure. ICES J. Mar. Sci. **62**(3): 397–404. doi:10.1016/j.icesjms.2004.07.030.

Jennings, S., and Kaiser, M.J. 1998. The effects of fishing on marine ecosystems. In Advances in marine biology. Edited by J.H.S. Blaxter, A.J. Southward, and P.A. Tyler. Academic Press. pp. 201–352. doi:10.1016/S0065-2881(08)60212-6.

Johnson, G.R., Shoup, D.E., and Boswell, K.M. 2019. Incorporating fish orientation into target strength–total length equations: Horizontal-Aspect target-Strength equations for gizzard shad *Dorosoma cepedianum*. Fish. Res. **218**: 155–165. doi:10.1016/j.fishres.2019.05.009.

Kang, D., Sadayasu, K., Mukai, T., Iida, K., Hwang, D., Sawada, K., and Miyashita, K. 2004. Target strength estimation of black porgy *Acanthopagrus schlegeli* using acoustic measurements and a scattering model. Fish. Sci. **70**(5): 819–828. doi:10.1111/j.1444-2906.2004.00875.x.

Kubečka, J. 1994. Simple model on the relationship between fish acoustical target strength and aspect for high-frequency sonar in shallow waters. J. Appl. Ichthyol. **10**(2–3): 75–81. doi:10.1111/j.1439-0426.1994.tb00146.x.

LGL Ecological Research Associates. 2019. Characterization of fish assemblages associated with offshore oil and gas platforms in the Gulf of Mexico. Report for Contract No. M16PC00005. doi:10.13140/RG.2.2.28322.25282.

Lilja, J., Marjomäki, T.J., Riikonen, R., and Jurvelius, J. 2000. Side-aspect target strength of Atlantic salmon (*Salmo salar*), brown trout (*Salmo trutta*), whitefish (*Coregonus lavaretus*), and pike (*Esox lucius*). Aquat. Living Resour. **13**(5): 355–360. doi:10.1016/S0990-7440(00)01072-X.

Love, R.H. 1971. Dorsal-aspect target strength of an individual fish. J. Acoust. Soc. Am. **49**(3B): 816–823. doi:10.1121/1.1912422.

MacLennan, D.N. 1990. Acoustical measurement of fish abundance. J. Acoust. Soc. Am. **87**(1): 1–15. doi:10.1121/1.399285.

MacLennan, D.N., Fernandes, P.G., and Dalen, J. 2002. A consistent approach to definitions and symbols in fisheries acoustics. ICES J. Mar. Sci. **59**(2): 365–369. doi:10.1006/jmsc.2001.1158.

Mason, J.E. 1998. Declining rockfish lengths in the Monterey Bay, California, recreational fishery, 1959–94. Mar. Fish. Rev. **60**(3): 15–28.

1268

Can. J. Fish. Aquat. Sci. Vol. 79, 2022

McClanahan, T.R., and Graham, N.A.J. 2005. Recovery trajectories of coral reef fish assemblages within Kenyan marine protected areas. Mar. Ecol. Prog. Ser. **294**: 241–248. doi:10.3354/meps294241.

McClatchie, S., Alsop, J., and Coombs, R.F. 1996a. A re-evaluation of relationships between fish size, acoustic frequency, and target strength. ICES J. Mar. Sci. **53**(5): 780–791. doi:10.1006/jmsc.1996.0099.

McClatchie, S., Alsop, J., Ye, Z., and Coombs, R.F. 1996b. Consequence of swimbladder model choice and fish orientation to target strength of three New Zealand fish species. ICES J. Mar. Sci. **53**(5): 847–862. doi:10.1006/jmsc.1996.0106.

Mehner, T. 2006. Prediction of hydroacoustic target strength of vendace (*Coregonus albula*) from concurrent trawl catches. Fish. Res. **79**(1): 162–169. doi:10.1016/j.fishres.2006.01.014.

Munnelly, R.T., Reeves, D.B., Chesney, E.J., and Baltz, D.M. 2021. Spatial and temporal influences of nearshore hydrography on fish assemblages associated with energy platforms in the northern Gulf of Mexico. Estuar. Coasts, **44**(1): 269–285. doi:10.1007/s12237-020-00772-7.

Nakken, O., and Olsen, K. 1977. Target strength measurements of fish. *In* ICES Symposium on Acoustic Methods in Fisheries Research. Vol. 24. ICES. pp. 52–69. Available from https://imr.brage.unit.no/imr-xmlui/handle/11250/107967 [accessed 30 March 2020].

Ogle, D.H., Wheeler, P., and Dinno, A. 2020. FSA: Fisheries Stock Analysis. R package version 0.8.31. Available from https://github.com/droglenc/FSA.

Ona, E., and Mitson, R.B. 1996. Acoustic sampling and signal processing near the seabed: the deadzone revisited. ICES J. Mar. Sci. **53**(4): 677–690. doi:10.1006/jmsc.1996.0087.

Parker-Stetter, S.L. 2009. Standard operating procedures for fisheries acoustic surveys in the Great Lakes. Great Lakes Fishery Commission. Available from https://agris.fao.org/agris-search/search.do?recordID=US201300139449 [accessed 25 September 2020].

Pope, J.G., and Knights, B.J. 1982. Comparison of length distributions of combined catches of all demersal fishes in surveys in the North Sea and at Faroe Bank. Can. Spec. Publ. Fish. Aquat. Sci. **59**: 116–118.

Priede, I.G., Bagley, P.M., Smith, A., Creasey, S., and Merrett, N.R. 1994. Scavenging deep demersal fishes of the Porcupine Seabight, north-east Atlantic: observations by baited camera, trap and trawl. J. Mar. Biol. Assoc. **74**(3): 481–498. doi:10.1017/S0025315400047615.

Reynolds, E.M., Cowan, J.H., Lewis, K.A., and Simonsen, K.A. 2018. Method for estimating relative abundance and species composition around oil and gas platforms in the northern Gulf of Mexico, U.S.A. Fish. Res. **201**: 44–55. doi:10.1016/j.fishres.2018.01.002.

Robinson, J.P.W., and Baum, J.K. 2016. Trophic roles determine coral reef fish community size structure. Can. J. Fish. Aquat. Sci. **73**(4): 496–505. doi:10.1139/cjfas-2015-0178.

Robinson, J.P.W., Williams, I.D., Edwards, A.M., McPherson, J., Yeager, L., Vigliola, L., et al. 2017. Fishing degrades size structure of coral reef fish communities. Global Change Biol. **23**(3): 1009–1022. doi:10.1111/gcb.13482. PMID:27564866.

Rudstam, L.G., Parker-Stetter, S.L., Sullivan, P.J., and Warner, D.M. 2009. Towards a standard operating procedure for fishery acoustic surveys in the Laurentian Great Lakes, North America. ICES J. Mar. Sci. **66**(6): 1391–1397. doi:10.1093/icesjms/fsp014.

Schuett, M.A., Ding, C., Kyle, G., and Shively, J.D. 2016. Examining the behavior, management preferences, and sociodemographics of artificial reef users in the Gulf of Mexico offshore from Texas. N. Am. J. Fish. Manage. **36**(2): 321–328. doi:10.1080/02755947.2015.1123204.

Scoulding, B., Gastauer, S., MacLennan, D.N., Fässler, S.M.M., Copland, P., and Fernandes, P.G. 2017. Effects of variable mean target strength on estimates of abundance: the case of Atlantic mackerel (*Scomber scombrus*). ICES J. Mar. Sci. **74**(3): 822–831. doi:10.1093/icesjms/fsw212.

Secor, D.H. 2015. Migration ecology of marine fishes. Johns Hopkins University Press, Md.

SEDAR. 2018. SEDAR 52 stock assessment report, Gulf of Mexico Red Snapper. Southeast Data, Assessment, and Review (SEDAR), North Charleston, South Carolina.

SEDAR. 2020. SEDAR 67 stock assessment report, Gulf of Mexico Vermilion Snapper. Southeast Data, Assessment, and Review (SEDAR), North Charleston, South Carolina.

Shin, Y.-J., Rochet, M.-J., Jennings, S., Field, J.G., and Gislason, H. 2005. Using size-based indicators to evaluate the ecosystem effects of fishing. ICES J. Mar. Sci. **62**(3): 384–396. doi:10.1016/j.icesjms.2005.01.004.

Simmonds, J., and MacLennan, D.N. 2008. Fisheries acoustics: theory and practice. John Wiley & Sons.

Simonsen, K. 2013. Reef fish demographics on Louisiana artificial reefs: the effects of reef size on biomass distribution and foraging dynamics. LSU doctoral dissertations. Available from https://digitalcommons.lsu.edu/gradschool_dissertations/160.

Sprules, W.G., and Barth, L.E. 2016. Surfing the biomass size spectrum: some remarks on history, theory, and application. Can. J. Fish. Aquat. Sci. **73**(4): 477–495. doi:10.1139/cjfas-2015-0115.

Stanley, D.R., and Wilson, C.A. 1997. Seasonal and spatial variation in the abundance and size distribution of fishes associated with a petroleum platform in the northern Gulf of Mexico. Can. J. Fish. Aquat. Sci. **54**(5): 1166–1176. doi:10.1139/f97-005.

Stunz, G.W., and Coffey, D.M. 2020. A review of the ecological performance and habitat value of standing versus reefed oil and gas platform habitats in the Gulf of Mexico. Available from https://tamucc-ir.tdl.org/handle/1969.6/89073 [accessed 28 September 2020].

Sweeting, C.J., Badalamenti, F., D'Anna, G., Pipitone, C., and Polunin, N.V.C. 2009. Steeper biomass spectra of demersal fish communities after trawler exclusion in Sicily. ICES J. Mar. Sci. **66**(1): 195–202. doi:10.1093/icesjms/fsn203.

Trebilco, R., Baum, J.K., Salomon, A.K., and Dulvy, N.K. 2013. Ecosystem ecology: size-based constraints on the pyramids of life. Trends Ecol. Evol. **28**(7): 423–431. doi:10.1016/j.tree.2013.03.008. PMID:23623003.

Trenkel, V.M., Ressler, P.H., Jech, M., Giannoulaki, M., and Taylor, C. 2011. Underwater acoustics for ecosystem-based management: state of the science and proposals for ecosystem indicators. Mar. Ecol. Prog. Ser. **442**: 285–301. doi:10.3354/meps09425.

Wanzenböck, J., Kubecka, J., Sajdlova, Z., and Frouzova, J. 2020. Hydroacoustic target strength vs. fish length revisited: Data of caged, free-swimming European whitefish (*Coregonus lavaretus* L.) suggest a bi-phasic linear relationship under a limited range of tilt angles. Fish. Res. **229**: 105620. doi:10.1016/j.fishres.2020.105620.

Wheeland, L.J., and Rose, G.A. 2016. Acoustic measures of lake community size spectra. Can. J. Fish. Aquat. Sci. **73**(4): 557–564. doi:10.1139/cjfas-2014-0446.

Wilson, S.K., Fisher, R., Pratchett, M.S., Graham, N.A.J., Dulvy, N.K., Turner, R.A., et al. 2010. Habitat degradation and fishing effects on the size structure of coral reef fish communities. Ecol. Appl. **20**(2): 442–451. doi:10.1890/08-2205.1. PMID:20405798.

Yurista, P.M., Yule, D.L., Balge, M., VanAlstine, J.D., Thompson, J.A., Gamble, A.E., et al. 2014. A new look at the Lake Superior biomass size spectrum. Can. J. Fish. Aquat. Sci. **71**(9): 1324–1333. doi:10.1139/cjfas-2013-0596.

Zhang, J., Chen, P.M., Chen, G.B., Fang, L.C., and Tang, Y. 2014. Acoustic target strength measurement of banded grouper (*Epinephelus awoara* (Temming and Schlegel, 1842)) and threadsial filefish (*Stephanolepis cirrhifer* (Temming & Schlegel, 1850)) in the South China Sea. J. Appl. Ichthyol. **29**(6): 63.